Environ. Sci. Technol. **2008,** *42,* 7301–7308

A Quantum Mechanical Study on the Formation of PCDD/Fs from 2-Chlorophenol as Precursor

QINGZHU ZHANG,* SHANQING LI, XIAOHUI QU, XIANGYAN SHI, AND WENXING WANG*

Environment Research Institute, Shandong University, Jinan 250100, P. R. China

Received June 11, 2008. Accepted August 01, 2008.. Revised manuscript received August 01, 2008

The most direct route to the formation of polychlorinated dibenzo-*p*-dioxins and dibenzofurans (PCDD/Fs) in combustion and thermal processes is the gas-phase reaction of chemical precursors such as chlorinated phenols. Detailed insight into the mechanism and kinetics properties is a prerequisite for understanding the formation of PCDD/Fs. In this paper, we carried out molecular orbital theory calculations for the homogeneous gas-phase formation of PCDD/Fs from 2-chlorophenol (2-CP). The profiles of the potential energy surface were constructed, and the possible formation pathways are discussed. The single-point energy calculation was carried out at the MPWB1K/6−311+G(3f,2p) level. Several energetically favorable formation pathways were revealed for the first time. The rate constants of crucial elementary steps were deduced over a wide temperature range of 600∼1200 K using canonical variational transition-state theory (CVT) with small curvature tunneling contribution (SCT). The rate-temperature formulas were fitted. The ratio of PCDD to PCDF formed shows strong dependency on the reaction temperature and chlorophenoxy radicals (CPRs) concentration.

1. Introduction

Polychlorinated dibenzo-*P*-dioxins (PCDDs) and dibenzofurans (PCDFs) have been at the forefront of public and regulatory concern because of their known toxicity, persistence and bioaccumulation. Major sources of PCDD/Fs in the environment are the combustion of waste materials as well as many other high-temperature processes commonly used in industrial settings. Reports of PCDD/F emissions from municipal waste incinerators have caused much public alarm and led to severe difficulties in constructing both municipal and hazardous waste incinerators.

The most direct route to the formation of PCDD/Fs is the gas-phase reaction of chemical precursors (*1*−*3*). Chlorophenols (CPs) are the most direct precursors of dioxin and among the most abundant aromatic compounds found in incinerator gas emissions (*4*−*6*). The homogeneous gas-phase formation of PCDD/Fs from CPs was suggested to make a significant contribution to the observed PCDD/F yields in full-scale incinerators (*7, 8*). The understanding of the reaction mechanism is crucial for any attempt to prevent PCDD/F formation. To obtain more insight into the actual formation pathways and explain the results of experimental observations, we initiated a theoretical study, employing a high-accuracy quantum chemical method, for the formation of PCDD/Fs using chlorophenol as precursor. Monochlorophenol (2-chlorophenol) was selected as a model precursor.

Formation of PCDD/Fs from the 2-chlorophenol (2-CP) precursor has been extensively studied experimentally, and continues to receive considerable attention. Evans (*9*) studied the thermal degradation of 2-CP under pyrolytic conditions. Dibenzo-p-dioxin (DD), dibenzofuran (DF), and 1-chlorodibenzo-p-dioxin (1-MCDD) were observed between 575 and 900 °C, but 4,6-dichlorodibenzofuran (4,6-DCDF) was not detected. In other work (*10*), Evans studied the oxidative degradation of 2-CP. Observed products in order of yield are as follows: 4,6-DCDF > DD > 1-MCDD, 4-MCDF, DF. In 2002, Sidhu and Edwards (*11*) investigated the role of phenoxy radicals in PCDD/Fs formation by studying the oxidation of 2-CP at different precursor concentrations: 4, 33, and 684 ppm. Observation shows that the concentration of radicals present in the oxidation system has a significant effect on the PCDD/F product distribution and ultimately the PCDD/PCDF ratio. The dominant PCDD/F product was found to be 1-MCDD at low inlet concentration (4 ppm) of 2-CP, whereas the major product of oxidation is 4,6-DCDF at high inlet concentration (33 and 684 ppm) of precursor. Several possible formation mechanisms were proposed to explain the observed products. In a recent paper, Altarawneh (*12*) carried out quantum chemical investigation into the formation mechanism of PCDD/Fs. Two pathways for molecule−molecule interactions, three pathways for molecule-radical interactions, and nine pathways for radical−radical interactions were investigated for the formation of DD, 1-MCDD, 4,6-DCDF, and 4-MCDF from the different possible combinations of 2-CP and 2-chlorophenoxy radical (2-CPR). The study of Altarawneh (*12*) indicated that 1-MCDD should be the favored product in 2-CP pyrolysis, in agreement with experimental findings. However, because the proposed formation pathways of 4,6-DCDF requires crossing a large activation barrier (53.0 and 48.1 kcal/mol), Altarawneh could not give a reasonable explanation of the experimental observation of Evans (*10*) that 4,6-DCDF is the major product under oxidative conditions.

The kinetic models that account for the contribution of the gaseous route in the production of PCDD/Fs in combustion processes use the rate constants of the elementary reactions (*13*). However, due to the absence of direct experimental and theoretical values, the rate constants of many elementary steps were assigned to be the values reported in the literature for analogous reactions (*13, 14*). However, where there are uncertainties, the numerical values have been adjusted somewhat to bias the mechanism in favor of PCDD/Fs formation, i.e., worst case modeling (*13, 14*). In this study, the rate constants of crucial elementary reactions, especially the controlling step in the dioxin formation, have been deduced using canonical variational transition-state theory (CVT) (*15*) with small curvature tunneling (SCT) (*16*) contribution.

2. Computational Methods

High-accuracy molecular orbital calculations were carried out using the Gaussian 03 package (*17*) on an SGI Origin 2000 supercomputer. The geometrical parameters were optimized at the MPWB1K/6-31+G(d,p) level. The MPWB1K method (*18*) is an HDFT model with excellent performance for thermochemistry, thermochemical kinetics, hydrogen bonding, and weak interactions. The vibrational frequencies

* Address correspondence to aither author. E-mail: zqz@sdu.edu.cn (Q.Z.); wxwang@sdu.edu.cn (W.W.). Fax: 86-531-8836 9788 (Q.Z. and W.W.).

10.1021/es801599n CCC: $40.75
Published on Web 09/04/2008

were also calculated at the same level in order to determine the nature of the stationary points, the zero-point energy (ZPE), and the thermal contributions to the free energy of activation. Each transition state was verified to connect the designated reactants with products by performing an intrinsic reaction coordinate (IRC) analysis (*19*). For a more accurate evaluation of the energetic parameters, a more flexible basis set, 6-311+G(3df,2p), was employed to determine the energies of the various species. By means of the Polyrate 9.3 program (*20*), direct dynamics calculations were carried out using the canonical variational transition state theory (CVT) (*15*) with small curvature tunneling contribution (SCT) (*16*).

3. Results and Discussion

To clarify the reliability of the theoretical calculations, we optimized the geometries and calculated the vibrational frequencies of phenol and chlorobenzene. The results at the MPWB1K/6-31+G(d,p) level agree well with the available experimental values, and the maximum relative error is less than 0.9% for the geometrical parameters and less than 8.0% for the vibrational frequencies. From this result, it might be inferred that the same accuracy could be expected for the species involved in the formation of PCDD/Fs from 2-CP. Furthermore, previous study shows that MPWB1K is an excellent method for prediction of transition state geometries (*18*).

3.1. Formation of 2-CPRs. The homogeneous gas-phase formation of PCDD/Fs from 2-CP was proposed that involve chlorophenoxy radical−radical coupling, radical−molecule recombination of chlorophenoxy and chlorophenol. Previous research (*12, 21*) has shown that the radical−molecule pathway requires chlorine and hydroxyl displacement as first steps, and these steps are not energetically favored. So the radical−molecule pathway is not competitive with the radical−radical pathway. The dimerization of 2-chlorophenoxy radicals (2-CPRs) is the major pathway for the formation of PCDD/Fs. Thus, we first studied the formation of 2-CPRs. In municipal waste incinerators, 2-CPRs can be formed through loss of the phenoxyl-hydrogen via unimolecular, bimolecular, or possibly other low-energy pathways (including heterogeneous reactions). The unimolecular reaction includes the decomposition of 2-CP with the cleavage of the O—H bond. The bimolecular reactions include attack by H or Cl under pyrolytic conditions and by H, OH, O (^{3}P) or Cl under high-temperature oxidative conditions.

For the unimolecular decomposition of 2-CP, breaking the O—H bond is a highly endothermic process. There is no transition state in the reaction because the potential curve is attractive along the O—H distance. The bimolecular reactions of 2-CP with H, OH, O (^{3}P), and Cl proceed via a direct hydrogen abstraction mechanism. The potential barriers (ΔE) and the reaction enthalpies (ΔH, 0 K) were calculated at the MPWB1K/6−311+G(3df,2p) level. For the reaction with Cl, the energy of the transition state without ZPE correction is 0.32 kcal/mol higher than the total energy of the reactants. However, the energy of the transition state including ZPE is 2.32 kcal/mol lower than the total energy of the reactants.

$$\text{2-CP} \rightarrow \text{2-CPR} + \text{H} \qquad \Delta H = 85.91 \text{ kcal/mol} \quad (1)$$

$$\text{2-CP} + \text{H} \rightarrow \text{2-CPR} + \text{H}_2 \qquad \Delta E = 13.80 \text{ kcal/mol}$$
$$\Delta H = -12.01 \text{ kcal/mol} \quad (2)$$

$$\text{2-CP} + \text{OH} \rightarrow \text{2-CPR} + \text{H}_2\text{O} \qquad \Delta E = 3.20 \text{ kcal/mol}$$
$$\Delta H = -26.91 \text{ kcal/mol} \quad (3)$$

$$\text{2-CP} + \text{O}(^3\text{P}) \rightarrow \text{2-CPR} + \text{OH} \qquad \Delta E = 7.51 \text{ kcal/mol}$$
$$\Delta H = -11.35 \text{ kcal/mol} \quad (4)$$

$$\text{2-CP} + \text{Cl} \rightarrow \text{2-CPR} + \text{HCl} \qquad \Delta E = -2.32 \text{ kcal/mol}$$
$$\Delta H = -14.96 \text{ kcal/mol} \quad (5)$$

3.2. Formation of PCDD/Fs from 2-CPRs. *3.2.1. Formation of PCDDs from 2-CPRs.* Three PCDD congeners, DD, 1-MCDD, and 1,6-DCDD, can be experimentally observed in the oxidation and pyrolysis of 2-CP (*9*−*11*). Four possible formation pathways, depicted in Figure 1a, are proposed for the formation of three dioxins in this study. The formation pathways involve four elementary processes: dimerization of 2-CPRs, Cl, or H abstraction, ring closure, and intra-annular elimination of Cl or H. In pathway 1 and pathway 3, the ring closure and elimination of Cl occur in a one-step reaction. All of the Cl or H abstraction processes are highly exothermic with low-energy barriers. The ring closure process involves a high barrier and is strongly endoergic, and it is the rate determining step for pathways 1 and 3. Unimolecular elimination of H is the kinetically controlling process for pathways 2 and 4 due to the high potential barrier. The thermodynamically favored routes to PCDDs formation are pathways 1 and 3. DD and 1-MCDD are the major PCDD products, in agreement with experimental findings (*9*−*12*).

The formation of DD and 1-MCDD were also studied by Altarawneh (*12*). For a comparison, the formation mechanism proposed by Altarawneh is presented in Figure 1b. Comparison of Figure 1a and b shows that the pathways proposed by Altarawneh (*12*) are similar to pathways 1 and 3. But two obvious differences were observed: (1) The coupling of the oxygen-centered radical mesomer with the ortho carbon−hydrogen centered radical mesomer requires crossing a potential barrier of 9.0 kcal/mol in the study of Altarawneh (*12*), whereas this process is barrierless in our study; (2) The potential barriers reported by Altarawneh are much lower than the values obtained by us for all of the Cl or H abstraction processes. For example, the potential barrier of Cl abstraction from IM1 (denoted as D8 in the study of Altarawneh (*12*)) by H atom is 0.7 kcal/mol in the study of Altarawneh (*12*), whereas the value we obtained is 6.69 kcal/mol. The discrepance may arise from the different calculation levels. The energies of Altarawneh (*12*) are calculated at the B3LYP level, while our energy calculations are carried out at the MPWB1K level. It is well-known that the B3LYP method systematically underestimates barrier heights (*18*). The kinetic calculations are most sensitive to the energies. In order to justify the performance of the MPWB1K method for the potential barriers, we have carried out additional potential barrier calculations employing higher level, G3MP2, for the Cl abstraction from IM1 by H atom. The G3MP2 calculation is rather expensive and extremely computationally demanding. It took more than 12 days to calculate the G3MP2 energy of TS1 on a personal computer with an Intel Core 2 Duo E6750 processor and 4GB main memory. The scratch file used up to 80 GB of disk space. The similar calculation using MPWB1K/6-311+G(3df,2p) requires less than 11 h. The two methods, MPWB1K/6-311+G(3df,2p) and G3MP2, produce consistent potential barriers within 0.9 kcal/mol.

In order to further compare with the formation mechanism proposed by Altarawneh (*12*), we checked the structures of reactants, transition states, intermediates, and products involved in the formation pathways of DD and 1-MCDD. Figure 2 shows the configurations of dimerization products (IM1 versus D8, IM2 versus D5), intermediates (IM3 versus preD3, IM5 versus preD5), and transition states (TS4 versus TS(preD3 → DD+Cl) located by Altarawneh (*12*) and us. The configurations of D8, preD3, D5, PreD5, and TS(preD3 → DD+Cl) are from the Cartesian coordinates offered by Altarawneh in the Supporting Information (*12*). It can be seen from Figure 2 that the configurations of IM1, IM2, IM3, and IM5 are obviously different from the configurations of D8, preD3, D5, and PreD5 (*12*). In IM1, IM2, IM3, and IM5, C(1) atom is at the cis-position of C(3) with respect to the C(2)—O bond, and C(2) atom is at the cis-position of C(4) atom with respect to the O—C(3) bond. This cis-configuration

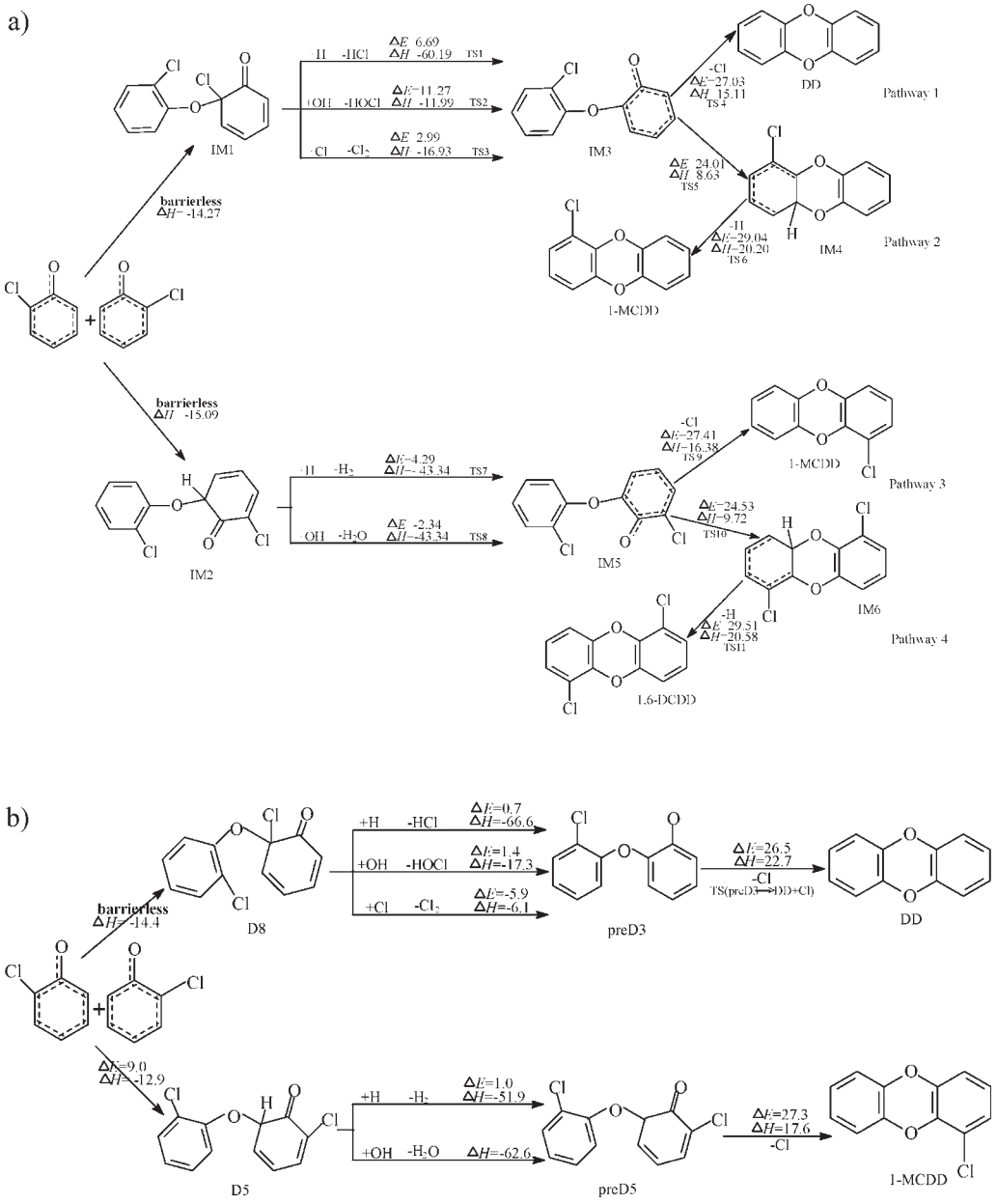

FIGURE 1. a. Formation routes of PCDDs from the 2-CP precursor. ΔH is calculated at 0 K. b. Formation routes of DD and 1-MCDD proposed by Altarawneh (*12*).

easily proceeds to the ring closure. However, in D8, preD3, D5, and PreD5, C(1) atom is at the trans-position of C(3), and C(2) atom is at the trans-position of C(4). The ring will be difficult to close from this trans-configuration due to the large steric hindrance. Figure 2 shows that the transition states (TS4 and TS(preD3 → DD+Cl)) of the ring closure process have the same configurations. The difference of the forming C(1)—O bond length (1.943 versus 1.935 Å) in the two transition states results from the different calculation levels. IRC calculation verified that the transition state (TS4 or TS(preD3 → DD+Cl)) connects to the intermediate IM3 not preD3. Therefore, the cis-formed IM1, IM2, IM3, and IM5 are reasonable intermediates for the formation of DD and 1-MCDD.

3.2.2. Formation of PCDFs from 2-CPRs. Experimental observation (*10*) shows that 4,6-DCDF is the major PCDF under oxidation of 2-CP. Two reaction routes were proposed by Altarawneh (*12*) to account for its formation. However, because the two formation routes require crossing large barriers (53.0 and 48.1 kcal/mol), Altarawneh could not give a reasonable explanation for the experimental observation of Evans (*10*) that 4,6-DCDF is the major product rather than DD and 1-MCDD under oxidative conditions. Therefore, there may be other possible 4,6-DCDF formation mechanisms. In this study, two new reaction pathways are proposed for the formation of 4,6-DCDF, as presented in Figure 3.

The first formation route involves five elementary steps: coupling of 2-CPRs, H abstraction by H atom or OH radical, tautomerization (H-shift), ring closure, and elimination of OH. The ortho−ortho coupling has a potential barrier of 8.27 kcal/mol. Both H abstraction processes have low barriers and are strongly exothermic. In the study of Altarawneh (*12*), the H-shift process has a significant barrier of 48.1 kcal/mol. In our study, H-shift could proceed via two different transition states: a five-membered ring transition state, denoted TS15, and a four-membered ring transition state, denoted TS16. The structures of TS15 and TS16 are shown in Figure 4. The energy of TS15 is 30.93 kcal/mol lower than that of TS16. Thus, the H-shift step via TS15 has a low potential barrier, only 18.45 kcal/mol. The ring closure process involves a high barrier of 29.17 kcal/mol and is strongly endoergic by 9.56

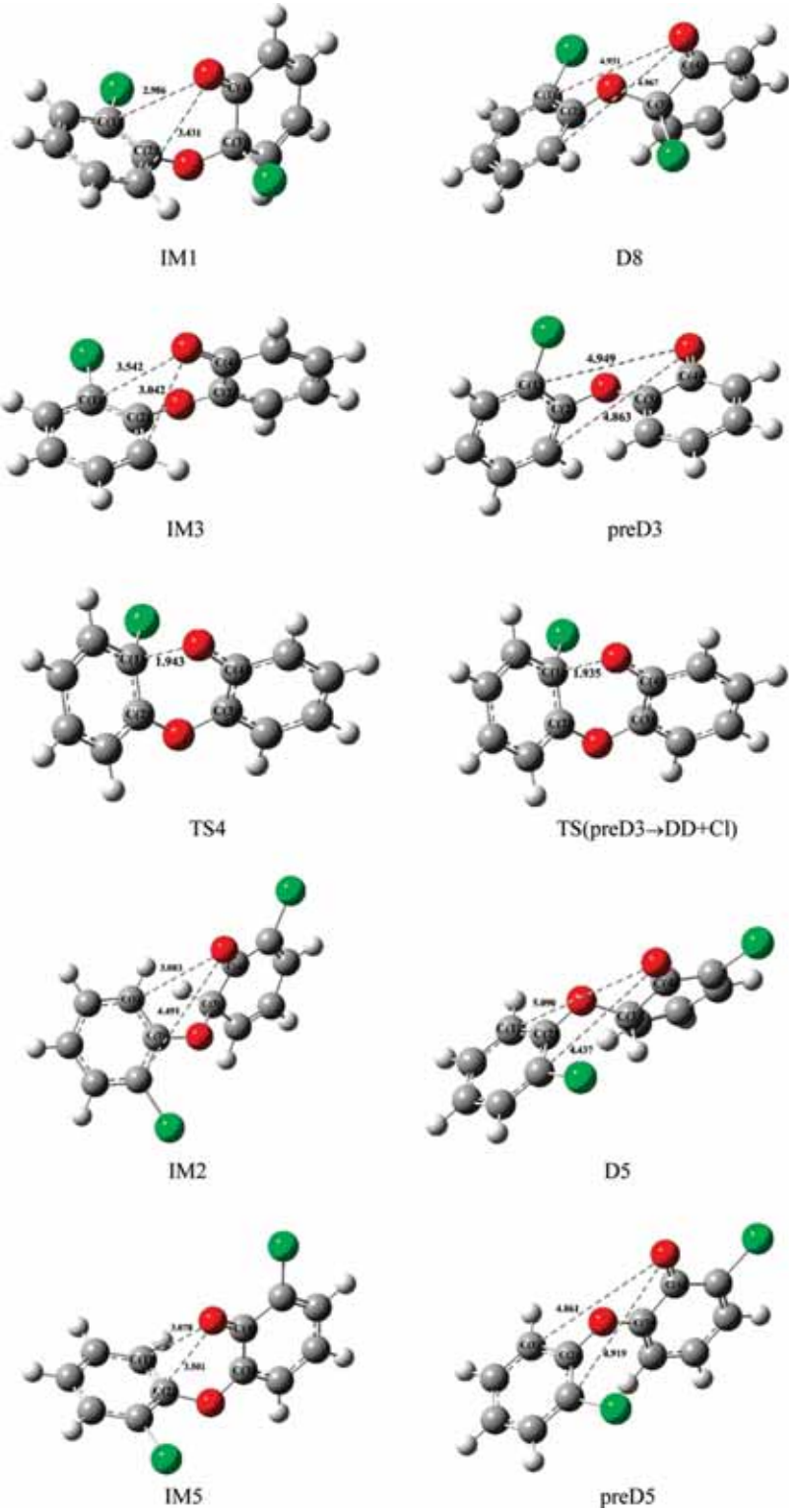

FIGURE 2. Configurations of dimerization products (IM1 versus D8, IM2 versus D5), intermediates (IM3 versus preD3, IM5 versus preD5), and transition states (TS4 versus TS(preD3 → DD+Cl)) located by Altarawneh and in this work.

kcal/mol, which is the rate controlling step for the formation of 4,6-DCDF in our study.

Similar to the first formation route of 4,6-DCDF, the second one also involves five elementary processes: dimerization of 2-CPRs, tautomerization (double H-transfer), H abstraction, ring closure, and OH desorption. In the study of Altarawneh (*12*), H transfer reactions from the keto−keto dimer IM7 to the enol−enol dimer IM11 involved two elementary steps. The first step is a single H atom transfer to the neighboring oxygen keto atom to form an enol−keto dimer. This process has a very high barrier of 53.0 kcal/mol. Transformation of the enol−keto dimer to the enol−enol dimer could proceed via two different energy barriers, 18.7 and 42.1 kcal/mol. In our study, the double hydrogen atom migration to the keto oxygen atoms can occur in a one-step reaction via the transition state TS19. The structure of TS19 is shown in Figure 4. The calculated vibrational frequencies contained only one imaginary component, 1546i cm^{-1}, confirming the first-order saddle point configuration. This concerted double hydrogen atom transfer process involves

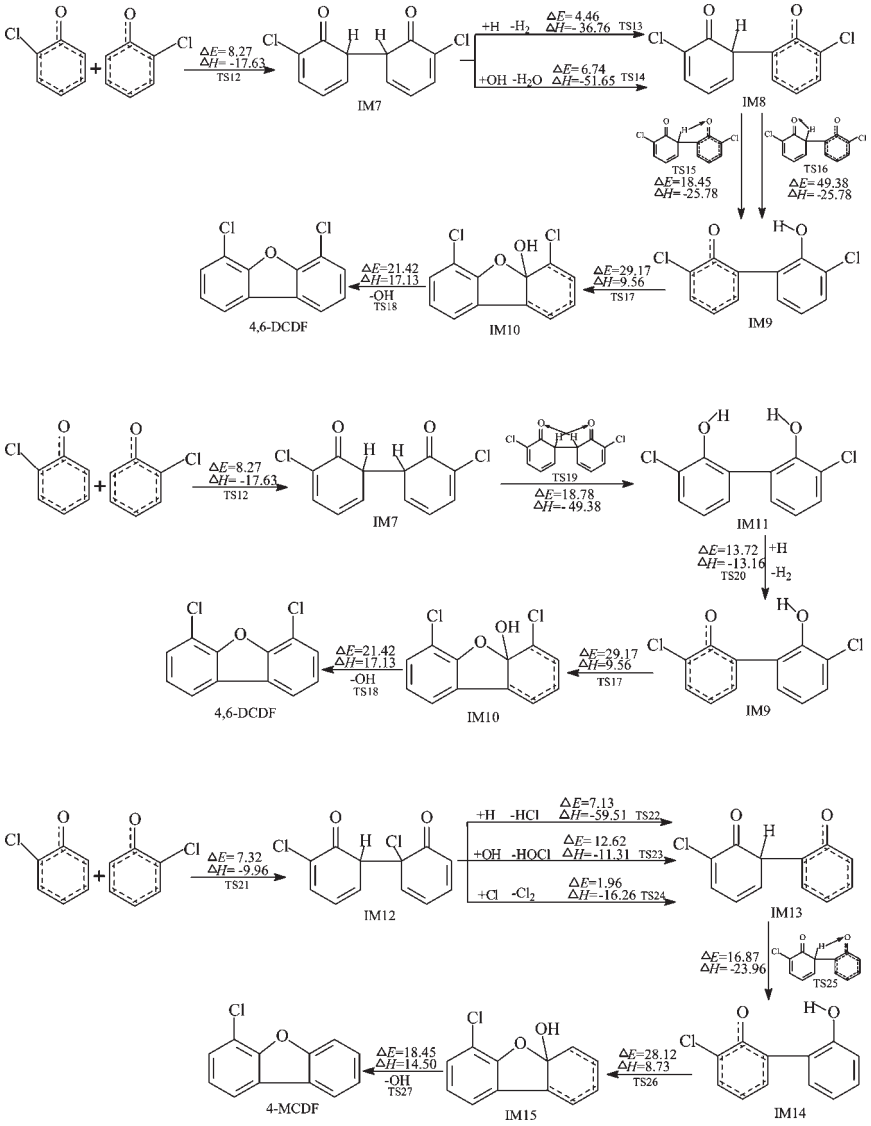

FIGURE 3. Formation routes of PCDFs from the 2-CP precursor. ΔH is calculated at 0 K.

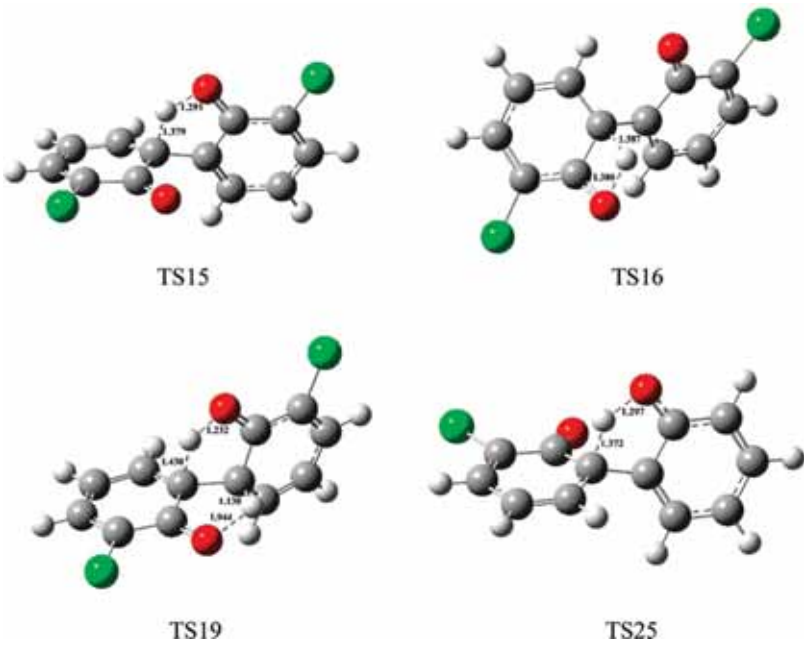

FIGURE 4. Configurations of the transition states of H-shift involved in the formation of PCDFs.

a barrier of 18.78 kcal/mol and is strongly exothermic by 49.38 kcal/mol. Altarawneh's study (*12*) shows that direct dehydration of the enol−enol dimer IM11 to form 4,6-DCDF is energetically unfavorable, with a very large barrier, 68.7 kcal/mol. In the combustion environment, active radicals will greatly facilitate H abstraction from the enol−enol dimer IM11. Then, 4,6-DCDF could be formed through ring closure and OH desorption reactions.

4-MCDF has been observed in the oxidation of 2-CP (*11*). A possible formation mechanism is proposed in this study. Similar to the formation of 4,6-DCDF, tautomerization from the keto−keto dimer to the enol−enol dimer requires crossing a high barrier of 47.7 kcal/mol in the study of Altarawneh (*12*), whereas the process has a low barrier of 16.87 kcal/mol in our study. Another possible formation route of 4-MCDF is the recombination of 2-chlorophenoxy radical with phenoxy radical.

The *o,o′*-dihydroxybiphenyl (DOHB) intermediate IM7 can be regarded as a prestructure for 4,6-DCDF, and IM12 is a prestructure of 4-MCDF. Figure 3 shows that the formation of IM7 is more exoergic than IM12 formation (by 7.67 kcal/mol at 0 K). Thus, IM7 is thermodynamically more stable than IM12. This can be explained by the steric effect. The coupling of two carbon (hydrogen)-centered radical mesomers forms IM7. IM12 is formed by the recombination of the carbon (hydrogen)-centered radical mesomer with the carbon (chlorine)-centered radical mesomer. Cl atom is larger than H atom, and has a larger steric effect. The sterically demanding formation of DOHB is inhibited by the voluminous chlorine atoms. If both ortho-positions of the phenol are substituted with chlorine, the formation of PCDFs is almost completely inhibited.

Comparison of Figure 1a and Figure 3 shows that the oxygen−carbon couplings appear to be barrierless, whereas the ortho−ortho couplings have a barrier of more than 7 kcal/mol. The preferred formation routes of DD and 1-MCDD involve three elementary steps. The formation pathways of 4,6-DCDF involve five elementary processes. Thus, the formation of PCDDs is preferred over the formation of PCDFs that is consistent with the experimental data: DD and 1-MCDD are the major dioxin products rather than 4,6-DCDF in the pyrolysis of 2-CP and are also major products of oxidation at low inlet concentration of precursor. However, at high inlet concentration of precursor, the dominant PCDD/F product is 4,6-DCDF under the oxidation conditions (*10, 11*). This can be explained by the concentration of 2-CPRs based on the study of Sidhu (*11*). At high inlet concentration of precursor and under the oxidation conditions, the carbon-centered mesomer of 2-CPR increases more than that of the oxygen-centered mesomer, as the carbon-centered mesomer is a more stable form of 2-CPR (*22*). Since PCDF formation involves only the more stable carbon-centered mesomer of 2-CPR, the increase in PCDF yields is more than the observed increase in PCDD.

3.3. Kinetics Calculations. Canonical variational transition state theory (CVT) (*15*) with small-curvature tunneling (SCT) (*16*) correction has been successfully performed for several analogous reactions (*23, 24*) and is an efficient method to calculate the rate constants. In this study, we used this method to calculate the rate constants of crucial elementary reactions over a wide temperature range of 600∼1200 K, which covers the possible formation temperature of PCDD/Fs in municipal waste incinerators. Due to the absence of the available experimental values, it is difficult to make a direct comparison of the calculated CVT/SCT rate constants with the experimental values for all the elementary reactions. An alternative approach to clarifying the reliability of the kinetics calculation is to compare the CVT/SCT rate constants with the available literature rate constant values for structurally similar compounds.

TABLE 1. Arrhenius Formulas (Units Are s^{-1} and cm^3 $Molecule^{-1}$ s^{-1} for Unimolecular and Bimolecular Reactions, Respectively) for Elementary Reactions Involved in the Formation of PCDD/Fs from the 2-CP Precursor over the Temperature Range of 600∼1200 K.

reactions	Arrhenius formulas
2-CP+H → 2-CPR+H_2	$k(T) = (1.10 \times 10^{-11})$ $\exp(-6437.64/T)$
2-CP+OH → 2-CPR+H_2O	$k(T) = (3.43 \times 10^{-12})$ $\exp(-2661.33/T)$
2-CP+O(^{3}P) → 2-CPR+OH	$k(T) = (4.75\times 10^{-12})$ $\exp(-3513.60/T)$
2-CP+Cl → 2-CPR+HCl	$k(T) = (2.09 \times 10^{-11})$ $\exp(118.87/T)$
IM1+H → IM3+HCl	$k(T) =(3.12 \times 10^{-12})$ $\exp(-2891.38/T)$
IM1+OH → IM3+HOCl	$k(T) = (1.02 \times 10^{-11})$ $\exp(-6442.22/T)$
IM1+Cl → IM3+Cl_2	$k(T) = (1.04 \times 10^{-11})$ $\exp(-1861.28/T)$
IM3 → DD+Cl	$k(T)= (3.58 \times 10^{11})$ $\exp(-13706.87/T)$
IM3 → IM4	$k(T) = (4.26 \times 10^{11})$ $\exp(-11885.95/T)$
IM4 → 1-MCDD+H	$k(T) = (2.35 \times 10^{13})$ $\exp(-15078.04/T)$
IM2+H → IM5+H_2	$k(T) = (2.00\times 10^{-20})$ $\exp(-2885.70/T)$
IM2+OH → IM5+H_2O	$k(T) = (6.81 \times 10^{-21})$ $\exp(-487.51/T)$
IM5 → 1-MCDD+Cl	$k(T) = (5.05 \times 10^{11})$ $\exp(-13763.30/T)$
IM5 → IM6	$k(T) = (3.74 \times 10^{9})$ $\exp(-6677.26/T)$
IM6 → 1,6-DCDD+H	$k(T) = (2.22 \times 10^{13})$ $\exp(-15257.27/T)$
2-CPR+2-CPR → IM7	$k(T) = (3.86 \times 10^{-15})$ $\exp(-5527.18/T)$
IM7+H → IM8+H_2	$k(T) = (1.28 \times 10^{-11})$ $\exp(-2222.77/T)$
IM7+OH → IM8+H_2O	$k(T) = (1.14 \times 10^{-12})$ $\exp(-4313.22/T)$
IM8 → IM9 via TS15	$k(T) = (1.39 \times 10^{9})$ $\exp(-2074.71/T)$
IM8 → IM9 via TS16	$k(T) = (6.28 \times 10^{3})$ $\exp(-5740.21/T)$
IM9 → IM10	$k(T) = (2.11 \times 10^{12})$ $\exp(-14722.61/T)$
IM10 → 4,6-DCDF	$k(T) = (4.11 \times 10^{13})$ $\exp(-11176.13/T)$
IM7 → IM11	$k(T) = (3.71 \times 10^{10})$ $\exp(-6831.91/T)$
IM11+H → IM9+H2	$k(T) = (1.25 \times 10^{-13})$ $\exp(-106.32/T)$
2-CPR+2-CPR → IM12	$k(T) = (1.56 \times 10^{-16})$ $\exp(-4904.96/T)$
IM12+H → IM13+HCl	$k(T) = (9.27 \times 10^{-12})$ $\exp(-4210.06/T)$
IM12+OH → IM13+HOCl	$k(T) = (7.35 \times 10^{-12})$ $\exp(-7395.10/T)$
IM12+Cl → IM13+Cl_2	$k(T)= (3.29 \times 10^{-11})$ $\exp(-2140.44/T)$
IM13 → IM14	$k(T) = (2.11 \times 10^{10})$ $\exp(-4657.53/T)$
IM14 → IM15	$k(T) = (2.04 \times 10^{12})$ $\exp(-14193.42/T)$
IM15 → 4-MCDF+OH	$k(T) = (2.34 \times 10^{13})$ $\exp(-9511.18/T)$

There are no previous data for the reactions of 2-CP+H → 2-CPR+H_2 and 2-CP+OH → 2-CPR+H_2O. So, the calculated rate constants were compared with the literature values (*25*−*27*) for phenol → C_6H_5O+H_2 and phenol+OH → C_6H_5O+H_2O, respectively. The CVT/SCT rate constants for

2-CP+H → 2-CPR+H_2 and 2-CP+OH → 2-CPR+H_2O are over 1 order of magnitude lower than the literature values (*25*−*27*) for phenol+H → C_6H_5O+H_2 and phenol+OH → C_6H_5O+H_2O, respectively. It is well-known that the chlorine substitution in the ortho position increases the strength of the O—H bond in chlorophenol and decreases its reactivity (*26*). The dissociation energies (0 K) of the O—H bonds in 2-CP and phenol are 85.91 and 83.95 kcal/mol. Thus, our CVT/SCT rate constants for 2-CP+H → 2-CPR+H_2 and 2-CP+OH → 2-CPR+H_2O are reasonable.

For the reactions with Cl atom, only one paper (*28*) is on record for the reactions of phenol, 2-CP, 3-CP, and 4-CP with Cl. At 296 K, the rate constant (*28*) for phenol+Cl → C_6H_5O+HCl is 1.93×10^{-10} cm^3 $molecule^{-1}$ s^{-1}. The values (*28*) for 3-CP+Cl → 3-CPR+HCl and 4-CP+Cl → 4-CPR+HCl are 1.56×10^{-10} and 2.37×10^{-10} cm^3 $molecule^{-1}$ s^{-1}. However, the value (*28*) for 2-CP+Cl → 2-CPR+HCl is 7.32×10^{-12} cm^3 $molecule^{-1}$ s^{-1}, which is much lower than those of the reactions of phenol, 3-CP and 4-CP with Cl. The CVT/SCT rate constant we calculated for 2-CP+Cl → 2-CPR+HCl is 4.29×10^{-11} cm^3 $molecule^{-1}$ s^{-1}, which is almost 6 times higher than the experimental value of 7.32×10^{-12} cm^3 $molecule^{-1}$ s^{-1}, but is lower than those of the reactions of phenol, 3-CP, and 4-CP with Cl. In order to check the reactivity and strength of the O—H bond in phenol and chlorophenols, we calculated the dissociation energy of the O—H bond. The values (0 K) are 83.95, 85.91, 85.01, and 82.76 kcal/mol for the O—H bond dissociation energy in phenol, 2-CP, 3-CP, and 4-CP, respectively. The O—H bond dissociation energy in 2-CP is only 0.9 kcal/mol higher than that in 3-CP. However, the experimental rate constant of 3-CP+Cl → 3-CPR+HCl is 21.31 times larger than that of 2-CP+Cl → 2-CPR+HCl (*28*). The dissociation energy of the O—H bond in 3-CP is 2.25 kcal/mol higher than that in 4-CP. The experimental rate constant of 4-CP+Cl → 4-CPR+HCl is only 1.52 times larger than that of the reaction of 3-CP+Cl → 3-CPR+HCl (*28*). It seems likely that the experiment underestimates the rate constant of the reaction of 2-CP+Cl → 2-CPR+HCl.

The unimolecular reactions involved in the formation of PCDD/Fs are the decomposition or the isomerization of the activated intermediates. There are no available experimental rate constants for the activated intermediates or structurally similar compounds, largely due to the short lifetime and the lack of efficient detection schemes for these activated species. Thus, it is difficult to make a comparison of the calculated CVT/SCT rate constants with the experimental values for the unimolecular decomposition or the isomerization of the activated intermediates. The CVT/SCT method has been successfully performed for many unimolecular reactions (*29*, *30*). Fernández-Ramos (*30*) calculated the rate constants for the dissociation and elimination channels in the thermal decomposition of methyl nitrite by direct dynamics method. In particular, the CVT/SCT calculations predicted rate constants that are in excellent agreement with those determined experimentally, indicating that the CVT/SCT method is able to predict reliable rate constants for the unimolecular reactions (*30*). We hope our CVT/SCT calculations may provide a good estimate for the crucial elementary reactions involved in the formation of PCDD/Fs from 2-CP.

Knowledge of the temperature dependence would be useful for the kinetic models (*13, 14*). The pre-exponential factor, the activation energy, and the rate constants are important input parameters in the kinetics models that account for the contribution of the gaseous route in the production of PCDD/Fs in combustion processes. Thus, the calculated CVT/SCT rate constants are fitted over the temperature range of 600∼1200 K and Arrhenius formulas are given in Table 1.

Acknowledgments

This work was supported by NSFC (National Natural Science Foundation of China, project no. 20507013, 20737001). We thank Professor Donald G. Truhlar for providing the POLYRATE 9.3 program. We also thank Dr. Pamela Holt for proofreading the manuscript.

Supporting Information Available

MPWB1K/6−31G(d,p) optimized geometries and calculated imaginary frequencies for the transition states involved in the formation of PCDD/Fs from 2-CP as precursor. The material is available free of charge via the Internet at http://pubs.acs.org.

Literature Cited

(1) Dickson, L. C.; Lenoir, D.; Hutzinger, O. Quantitative comparison of de novo and precursor formation of polychlorinated dibenzo-p-dioxins under simulated municipal solid waste incinerator postcombustion conditions. *Environ. Sci. Technol.* **1992**, *26*, 1822–1828.

(2) Addink, R.; Olie, K. Mechanisms of formation and destruction of polychlorinated dibenzo-p-dioxins and dibenzofurans in heterogeneous systems. *Environ. Sci. Technol.* **1995**, *29*, 1425–1435.

(3) Milligan, M. S.; Altwicker, E. R. Chlorophenol reactions on fly ash. 1. Adsorption/desorption equilibria and conversion to polychlorinated dibenzo-*p*-dioxins. *Environ. Sci. Technol.* **1996**, *30*, 225–229.

(4) Karasek, F. W.; Dickson, L. C. Model studies of polychlorinated dibenzo-p-dioxin formation during municipal refuse incineration. *Science* **1987**, *237*, 754–756.

(5) Shaub, W. M.; Tsang, W. Dioxin formation in incinerators. *Environ. Sci. Technol.* **1983**, *17*, 721–730.

(6) Altwicker, E. R. Relative rates of formation of polychlorinated dioxins and furans from precursor and de novo reactions. *Chemosphere* **1996**, *33*, 1897–1904.

(7) Hung, H.; Buekens, A. Comparison of dioxin formation levels in laboratory gas-phase flow reactors with those calculated using the Shaub-Tsang mechanism. *Chemosphere* **1999**, *38*, 1595–1602.

(8) BabushokV. TsangW. 7th International Congress on Combustion By-Products: Origins, Fate, and Health Effects, Research Triangle Park, North Carolina, 2001; p 36.

(9) Evans, C. S.; Dellinger, B. Mechanisms of dioxin formation from the high-temperature pyrolysis of 2-chlorophenol. *Environ. Sci. Technol.* **2003**, *37*, 1325–1330.

(10) Evans, C. S.; Dellinger, B. Mechanisms of dioxin formation from the high-temperature oxidation of 2-chlorophenol. *Environ. Sci. Technol.* **2005**, *39*, 122–127.

(11) Sidhu, S.; Edwards, P. Role of phenoxy radicals in PCDD/F formation. *Int. J. Chem. Kinet.* **2002**, *34*, 531–541.

(12) Altarawneh, M.; Dlugogorski, B. Z.; Kennedy, E. M.; Mackie, J. C. Quantum chemical investigation of formation of polychlorodibenzo-p-dioxins and dibenzofurans from oxidation and pyrolysis of 2-chlorophenol. *J. Phys. Chem. A* **2007**, *111*, 2563–2573.

(13) Shaub, W. M.; Tsang, W. Dioxin formation in incinerators. *Environ. Sci. Technol.* **1983**, *17*, 721–730.

(14) Khachatryan, L.; Asatryan, R.; Dellinger, B. Development of expanded and core kinetic models for the gas phase formation of dioxins from chlorinated phenols. *Chemosphere* **2003**, *52*, 695–708.

(15) Baldridge, M. S.; Gordor, R.; Steckler, R.; Truhlar, D. G. Ab initio reaction paths and direct dynamics calculations. *J. Phys. Chem.* **1989**, *93*, 5107–5119.

(16) Liu, Y,-P.; Lynch, G. C.; Truong, T. N.; Lu, D.-H.; Truhlar, D. G.; Garrett, B. C. Molecular modeling of the kinetic isotope effect for the [1,5]-sigmatropic rearrangement of cis-1,3-pentadiene. *J. Am. Chem. Soc.* **1993**, *115*, 2408–2415.

(17) Frisch, M. J.; Trucks, G. W.; Schlegel, H. B.; Scuseria, G. E.; Robb, M. A.; Cheeseman, J. R.; Montgomery, J. A., Jr.; Vreven, T.; Kudin, K. N.; Burant, J. C.; Millam, J. M.; Iyengar, S. S.; Tomasi, J.; Barone, V.; Mennucci, B.; Cossi, M.; Scalmani, G.; Rega, N.; Petersson, G. A.; Nakatsuji, H.; Hada, M.; Ehara, M.; Toyota, K.; Fukuda, R.; Hasegawa, J.; Ishida, M.; Nakajima, T.; Honda, Y.; Kitao, O.; Nakai, H.; Klene, M.; Li, X.; Knox, J. E.; Hratchian, H. P.; Cross, J. B.; Bakken, V.; Adamo, C.; Jaramillo, J.; Gomperts, R.; Stratmann, R. E.; Yazyev, O.; Austin, A. J.; Cammi, R.; Pomelli, C.; Ochterski, J. W.; Ayala, P. Y.; Morokuma, K.; Voth, G. A.;

Salvador, P.; Dannenberg, J. J.; Zakrzewski, V. G.; Dapprich, S.; Daniels, A. D.; Strain, M. C.; Farkas, O.; Malick, D. K.; Rabuck, A. D.; Raghavachari, K.; Foresman, J. B.; Ortiz, J. V.; Cui, Q.; Baboul, A. G.; Clifford, S.; Cioslowski, J.; Stefanov, B. B.; Liu, G.; Liashenko, A.; Piskorz, P.; Komaromi, I.; Martin, R. L.; Fox, D. J.; Keith, T.; Al-Laham, M. A.; Peng, C. Y.; Nanayakkara, A.; Challacombe, M.; Gill, P. M. W.; Johnson, B.; Chen, W.; Wong, M. W.; Gonzalez, C.; Pople, J. A. *Gaussian 03*, revision C.02; Gaussian, Inc.: Wallingford, CT, 2004.

(18) Zhao, Y.; Truhlar, D. G. Hybrid meta density functional theory methods for therochemistry, thermochemical kinetics, and noncovalent interactions: the MPW1B95 and MPWB1K models and comparative assessments for hydrogen bonding and van der waals interactions. *J. Phys. Chem. A* **2004**, *108*, 6908–6918.

(19) Fukui, K. The path of chemical reactions - the IRC approach. *Acc. Chem. Res.* **1981**, *14* (12), 363–368.

(20) Steckler, R.; Chuang, Y. Y.; Fast, P. L.; Corchade, J. C.; Coitino, E. L.; Hu, W. P.; Lynch, G. C.; Nguyen, K.; Jackells, C. F.; Gu, M. Z.; Rossi, I.; Clayton, S.; Melissas, V.; Garrett, B. C.; Isaacson, A. D.; Truhlar, D. G. *POLYRATE Version 9.3*; University of Minnesota: Minneapolis., 2002.

(21) Louw, R.; Ahonkhai, S. I. Radical/radical va radical/molecule reactions in the formation of PCdd/Fs from (chloro)phenols in incinerators. *Chemosphere* **2002**, *46*, 1273–1278.

(22) Mackie, J. C.; Doolan, K. R.; Nelson, P. F. Kinetics of the thermal decomposition of methoxybenzene (anisole). *J. Phys. Chem.* **1989**, *93*, 664–670.

(23) Zhang, Q.-Z.; Gu, Y.-S.; Wang, S.-K. Theoretical studies on the variational transitional state theory rate constants for the hydrogen abstraction reaction of O (^{3}P) with CH_3Cl and CH_2Cl_2. *J. Chem. Phys.* **2003**, *119*, 4339–4345.

(24) Zhang, Q.-Z.; Gu, Y.-S.; Wang, S.-K. Theoretical investigation on the mechanism and thermal rate constants for the reaction of atomic O (^{3}P) with CHF_2Cl. *J. Phys. Chem. A* **2003**, *107*, 3069–3075.

(25) Baulch, D. L.; Cobos, C. J.; Cox, R. A.; Esser, C.; Frank, P.; Just, Th.; Kerr, J. A.; Pilling, M. J.; Troe, J.; Walker, R. W.; Warnatz, J. Evaluated kinetic data for combustion modelling. *J. Phys. Chem. Ref. Data* **1992**, *21*, 411–429.

(26) Han, J.; Deming, R. L.; Tao, F. —M. Theoretical study of molecular structures and properties of the complete series of chlorophenols. *J. Phys. Chem. A* **2004**, *108*, 7736–7743.

(27) He, Y. Z.; Mallard, W. G.; Tsang, W. Kinetics of hydrogen and hydroxyl radical attack on phenol at high temperatures. *J. Phys. Chem.* **1988**, *92*, 2196–2201.

(28) Platz, J.; Nielsen, O. J.; Wallington, T. J.; Ball, J. C.; Hurley, M. D.; Straccia, A. M.; Schneider, W. F.; Sehested, J. Atmospheric chemistry of the phenoxy radical, C_6H_5O: UV spectrum and kinetics of its reaction with NO, NO_2, and O_2. *J. Phys. Chem. A* **1998**, *102*, 7964–7974.

(29) Luo, Q.; Li, Q. —S. Direct ab initio dynamics study of the unimocular reaction of CH_2FO. *J. Phys. Chem. A* **2004**, *108*, 5050–5056.

(30) Antonio, F.-R.; Emilio, M. —N.; Rios, M. A.; Jesus, R. —O.; Vazquez, S. A.; Estevez, C. M. Direct dynamics study of the dissociation and elimination channels in the thermal decomposition of methyl nitrite. *J. Am. Chem. Soc.* **1998**, *120*, 7594–7601.

ES801599N